

Expanded View Figures

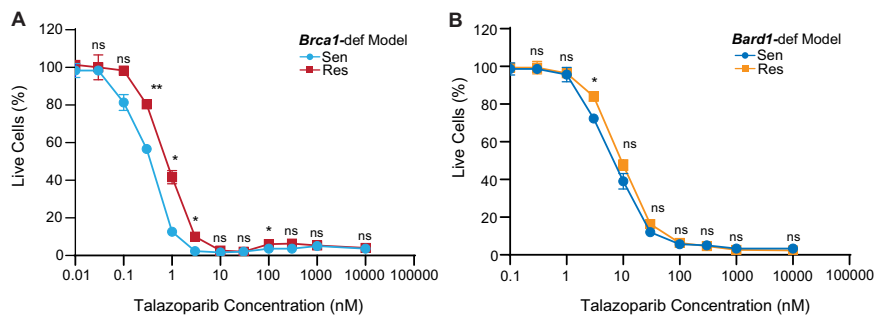


Figure EV1. Modest differences in talazoparib sensitivity observed in vitro compared to in-vivo settings (Fig. 1) in *Brca1*-def and *Bard1*-def breast tumor cells.

(A, B) In vitro cell viability assay comparing the talazoparib sensitivity between talazoparib-sensitive (“Sen”) *Brca1*-def and *Bard1*-def breast tumor cells and their talazoparib-resistant (“Res”) derivative lines. Cell viability values are normalized to the DMSO-treated control (considered as 100% live cells) and presented as mean values \pm SEM. *P* values were determined by a two-tailed, unpaired, Welch’s test. For the *Brca1*-def model, $n = 3$ for each concentration tested, ** at 0.3 nM indicates $P = 0.0028$, * at 1 nM indicates $P = 0.0104$, * at 3 nM indicates $P = 0.0104$, and * at 100 nM indicates $P = 0.0357$. For the *Bard1*-def model, $n = 3$ for each tested concentration, and * at 3.0 nM indicates $P = 0.0256$. ns; not significant.

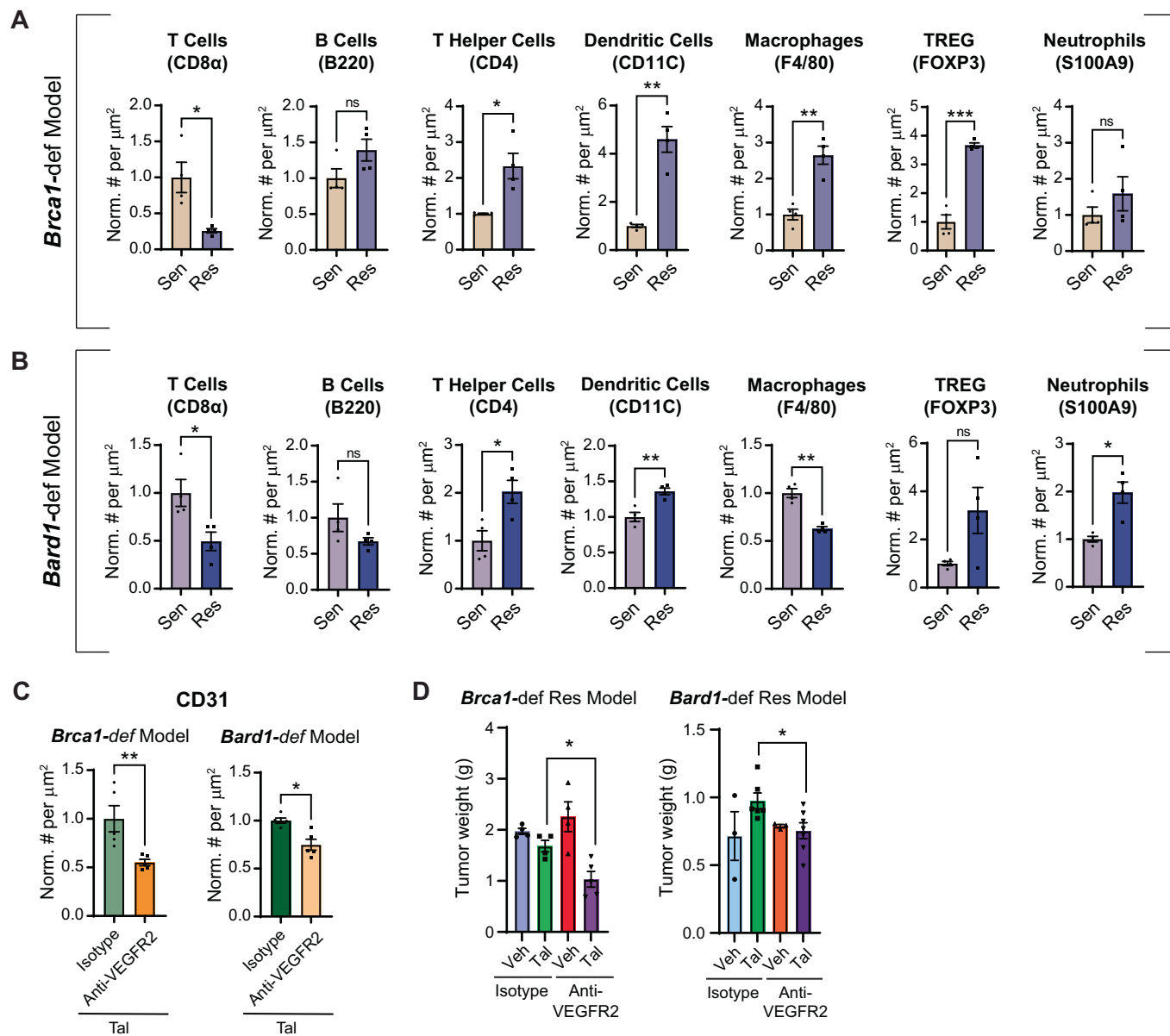
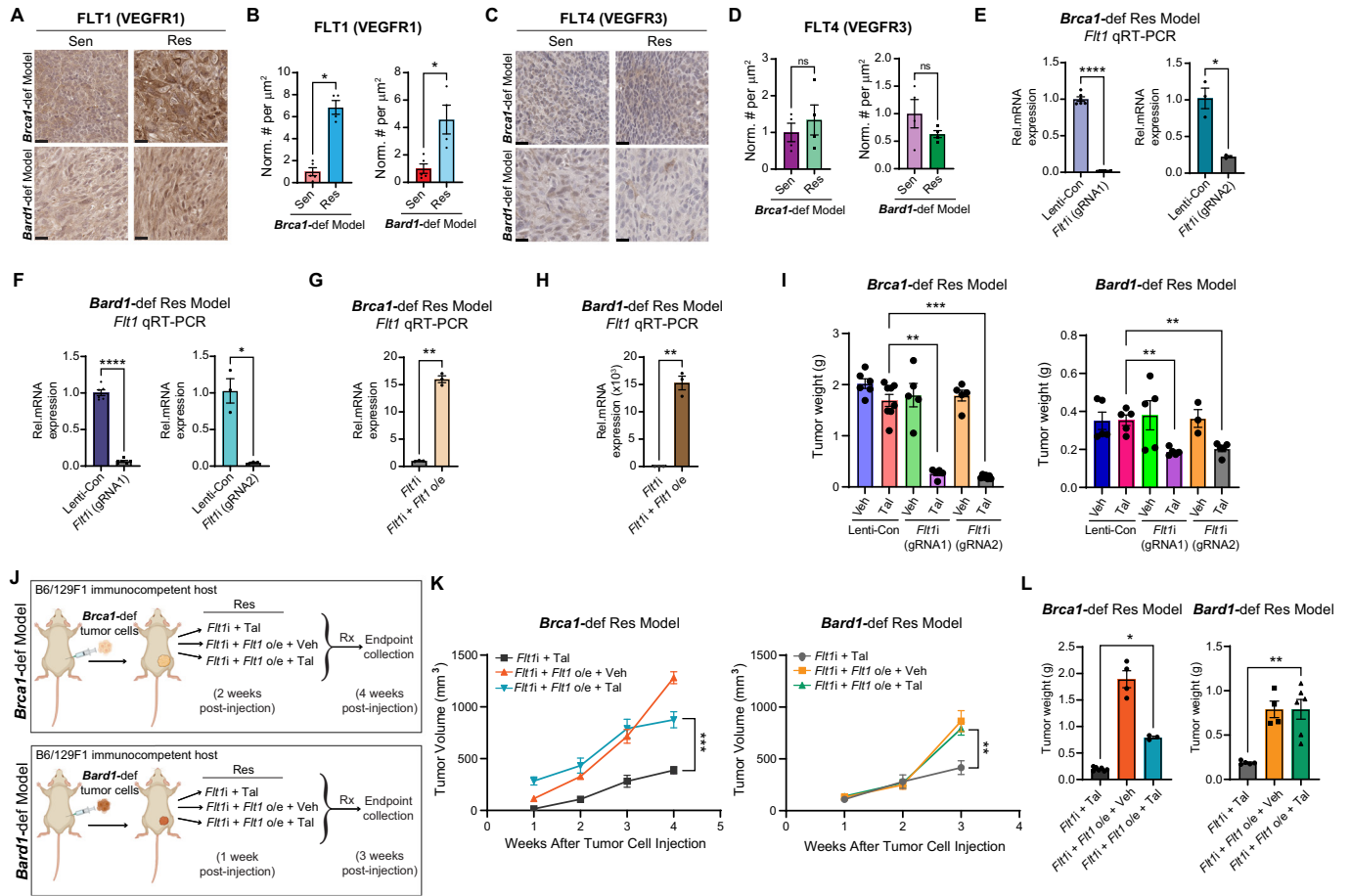


Figure EV2. Quantification of angiogenesis and immune-cell composition in *Brca1*-def and *Bard1*-def mutant breast tumors by immunostaining analysis.

(A, B) Immunostained tumor sections from Fig. 1 were quantified using automated QuPath software to identify positively stained cells. Data were presented as mean values \pm SEM. *P* values were determined by a two-tailed, unpaired, Welch's test. *n* = 4 mice for talazoparib-sensitive ("Sen") and -resistant ("Res") groups from both models. *P* values are listed in parentheses following the protein analyzed. For the *Brca1*-def model in (A): CD8 α (0.0375), CD4 (0.0329), CD11C (0.0061), F4/80 (0.0027), and FOXP3 (0.0007). For the *Bard1*-def model in (B), CD8 α (0.0293), CD4 (0.0186), CD11C (0.0048), F4/80 (0.0016), FOXP3 (ns), and S100A9 (0.0182). ns; not significant. (C) Quantitation of immunostained Res tumor sections using antibodies against CD31 (see treatments in Fig. 2I–K) using automated QuPath software to identify positively stained cells. *n* = 5 mice from both groups from both models. Data were presented as mean values \pm SEM. *P* values were determined by a two-tailed, unpaired, Mann-Whitney test. ** indicates *P* = 0.0079 for the *Brca1*-def model, and * indicates 0.0159 for the *Bard1*-def model. (D) Tumor weights from Fig. 2J were plotted after collection at endpoint. For the *Brca1*-def model, *n* = 4 tumors for the Isotype + Veh group, *n* = 4 tumors for the Isotype + Tal group, *n* = 4 tumors for the Anti-VEGFR2 + Veh group, and *n* = 5 tumors for the anti-VEGFR2 + Tal group. For the *Bard1*-def model, *n* = 3 tumors for Isotype + Veh group, *n* = 6 tumors for Isotype + Tal group, *n* = 3 tumors for anti-VEGFR2 + Veh group, and *n* = 7 tumors for anti-VEGFR2 + Tal group. Data were presented as mean values \pm SEM. *P* values were determined by a two-tailed, unpaired, Student's *t*-test, comparing endpoint tumor weights between the Isotype + Tal and anti-VEGFR2 + Tal groups. * indicates *P* = 0.0141 for the *Brca1*-def model, and * indicates *P* = 0.0222 for the *Bard1*-def model.



◀ **Figure EV3. FLT1 promotes PARPi-resistance in the *Brca1*-def and *Bard1*-def breast cancer models.**

(A) Representative images of IHC for total FLT1 expression in tumor sections from the mice described in Fig. 1. Scale bars, 20 μ m. (B) Immunostained sections from (A) were quantified using automated QuPath software to identify positively stained cells. $n = 5$ talazoparib-sensitive (“Sen”) tumors, and $n = 4$ talazoparib-resistant (“Res”) tumors from both *Brca1*-def and *Bard1*-def models. Data were presented as mean values \pm SEM. P values were determined by a two-tailed, unpaired, Mann-Whitney test. * indicates $P = 0.0159$ for both models. (C), Representative images of IHC for FLT4 in tumor sections from Fig. 1. Scale bars, 20 μ m. (D) Immunostained sections from (C) were quantified using automated QuPath software to identify positively stained cells. $n = 4$ Sen and Res tumors for both *Brca1*-def and *Bard1*-def models. Data were presented as mean values \pm SEM. P values were determined by a two-tailed, unpaired, Welch’s test. ns; not significant. (E) qRT-PCR results of *Flt1* repression of the indicated groups in the *Brca1*-def model for both gRNAs. $n = 6$ (consisting of two independent experiments for each triplicate testing) for both Lenti-Con and *Flt1i* for gRNA1 and $n = 3$ (one triplicate testing) for both Lenti-Con and *Flt1i* for gRNA2. Data were presented as mean values \pm SEM. P values were determined by a two-tailed, unpaired, Welch’s test: **** indicates $P < 0.0001$ for gRNA1 and * indicates $P = 0.0285$ for gRNA2. (F) qRT-PCR results of *Flt1* repression of the indicated groups in the *Bard1*-def model. $n = 6$ (two independent triplicate testing) for both Lenti-Con and *Flt1i* for gRNA1 and $n = 3$ (one triplicate testing) for both Lenti-Con and *Flt1i* for gRNA2. Data were presented as mean values \pm SEM. P values were determined by a two-tailed, unpaired, Welch’s test: **** indicates $P < 0.0001$ for gRNA1 and * indicates $P = 0.0273$ for gRNA2. (G) qRT-PCR results of *Flt1* expression of the indicated groups in the *Brca1*-def model. $n = 3$ (one triplicate testing) for *Flt1i* and *Flt1i* + *Flt1* overexpression (“o/e”) groups. Data were presented as mean values \pm SEM. P values were determined by a two-tailed, unpaired, Welch’s test: ** indicates $P = 0.0016$. (H) qRT-PCR results of *Flt1* expression of the indicated groups in the *Bard1*-def model. $n = 3$ (one triplicate testing) for *Flt1i* and *Flt1i* + *Flt1* o/e groups. Data were presented as mean values \pm SEM. P values were determined by a two-tailed, unpaired, Welch’s test: ** indicates $P = 0.0067$. (I) Tumor weights from Fig. 3D were plotted at endpoint. For the *Brca1*-def model, $n = 6$ tumors for Lenti-Con + Veh, $n = 8$ tumors for Lenti-Con + Tal, $n = 5$ tumors for *Flt1i* (gRNA1) + Veh or Tal and *Flt1i* (gRNA2) + Veh, and $n = 7$ tumors for *Flt1i* (gRNA2) + Tal treatment groups. For the *Bard1*-def model, $n = 5$ tumors for Lenti-Con + Veh or Tal, *Flt1i* (gRNA1) + Veh or Tal, and *Flt1i* (gRNA2) + Tal, and $n = 3$ tumors for *Flt1i* (gRNA2) + Veh. Data were presented as mean values \pm SEM. P values were determined by a two-tailed, unpaired, Mann-Whitney test, comparing endpoint tumor weights between Lenti-Con + Tal and *Flt1i* (gRNA1 or gRNA2) + Tal groups. For the *Brca1*-def model, ** indicates $P = 0.0016$ between Lenti-Con + Tal and *Flt1i* (gRNA1) + Tal and *** indicates $P = 0.0003$ between Lenti-Con + Tal and *Flt1i* (gRNA2) + Tal. For the *Bard1*-def model, ** indicates $P = 0.0079$ between Lenti-Con + Tal and *Flt1i* (gRNA1 or gRNA2) + Tal. (J) Schematic representation of the experiment designed to test whether *Flt1* re-expression rescues talazoparib-resistance in *Brca1*-def and *Bard1*-def mammary tumors with *Flt1* repression. The generation of *Brca1*- and *Bard1*-def cancer cells were described in Fig. 3. To stably re-express *Flt1*, we transduced *Flt1*-repressed cells with lentiviral particles carrying *Flt1* cDNA. For the *Brca1*-def model, randomized mice received either vehicle (“Veh”) or talazoparib (“Tal”) treatment starting at 2 weeks after tumor-cell injection and were euthanized at 4 weeks following injection. For the *Bard1*-def model, randomized mice received treatment at 1 week after tumor-cell injection and were euthanized at 3 weeks following injection. (K) Tumor growth curves comparing *Flt1i* + Tal and *Flt1i*-*Flt1* o/e + Veh or Tal. For the *Brca1*-def model, $n = 7$ mice for *Flt1i* + Tal, $n = 4$ mice for *Flt1i*-*Flt1* + o/e + Veh, and $n = 3$ mice for *Flt1i*-*Flt1* + o/e + Tal. For the *Bard1*-def model, $n = 5$ mice for *Flt1i* + Tal, $n = 4$ mice for *Flt1i*-*Flt1* + o/e + Veh, and $n = 6$ mice for *Flt1i*-*Flt1* + o/e + Tal. Data were presented as mean values \pm SEM. P values were determined with a one-way ANOVA test, comparing endpoint tumor volumes between the *Flt1i* + Tal and *Flt1i*-*Flt1* + o/e + Tal groups. For the *Brca1*-def model, *** at 4 weeks indicates $P = 0.0001$ and for the *Bard1*-def model, ** at 3 weeks indicates $P = 0.0074$. (L) Tumor weights from K were plotted at endpoint. For the *Brca1*-def model, $n = 7$ tumors for *Flt1i* + Tal, $n = 4$ tumors for *Flt1i*-*Flt1* + o/e + Veh, and $n = 3$ tumors for *Flt1i*-*Flt1* + o/e + Tal. For the *Bard1*-def model, $n = 5$ tumors for *Flt1i* + Tal, $n = 4$ tumors for *Flt1i*-*Flt1* + o/e + Veh, and $n = 6$ tumors for *Flt1i*-*Flt1* + o/e + Tal. Data were presented as mean values \pm SEM. P values were determined by a two-tailed, unpaired, Mann-Whitney test, comparing endpoint tumor weights between the *Flt1i* + Tal and *Flt1i*-*Flt1* + o/e + Tal groups. For the *Brca1*-def model, * indicates $P = 0.0167$ and for the *Bard1*-def model, ** indicates $P = 0.0043$.

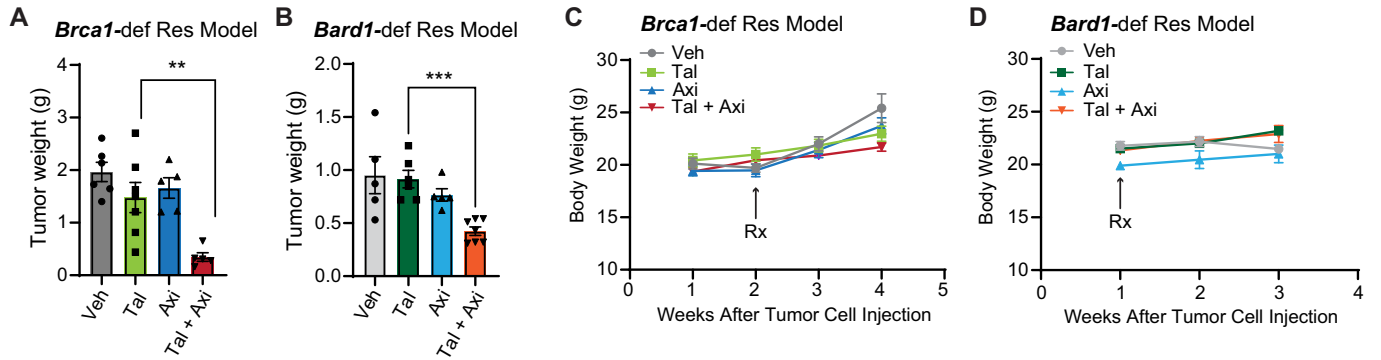


Figure EV4. Tumor and body weight analysis of mice treated with vehicle (“Veh”), talazoparib (“Tal”), and/or axitinib (“Axi”).

(A) Tumor weights from Fig. 4B were plotted at endpoint. $n = 6$ Veh-treated tumors, $n = 7$ Tal-treated tumors, $n = 5$ Axi-treated tumors, and $n = 5$ tumors treated with Tal + Axi. Data were presented as mean values \pm SEM. P values were determined by a two-tailed, unpaired, Mann-Whitney test, comparing endpoint tumor weights between the Tal and Tal + Axi groups. ** indicates $P = 0.0051$. (B) Tumor weights from Fig. 4E were plotted after collection at endpoint. $n = 5$ Veh-treated tumors, $n = 6$ Tal-treated tumors, $n = 5$ Axi-treated tumors, and $n = 7$ tumors treated with Tal + Axi. Data were presented as mean values \pm SEM. P values were determined by a two-tailed, unpaired Mann-Whitney test comparing endpoint tumor weights between the Tal and Tal + Axi groups. *** indicates $P = 0.0006$. (C, D) Body weight from treatment initiation until endpoint from Fig. 4A, D for each experiment. For the *Brca1*-def model, $n = 6$ Veh-treated tumors, $n = 7$ Tal-treated tumors, $n = 5$ Axi-treated tumors, and $n = 5$ tumors treated with Tal + Axi. For the *Bard1*-def model, $n = 5$ Veh-treated tumors, $n = 6$ Tal-treated tumors, $n = 5$ Axi-treated tumors, and $n = 7$ tumors treated with Tal + Axi.

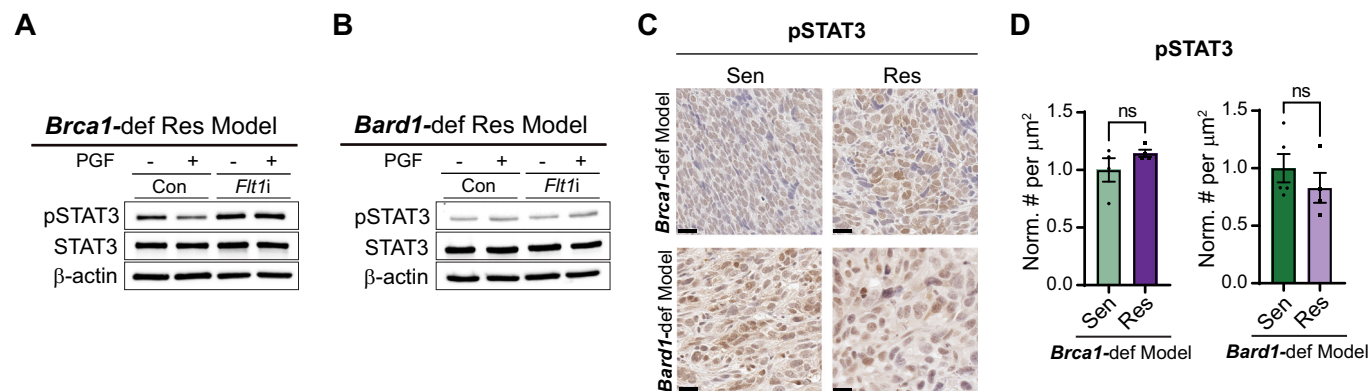


Figure EV5. Quantitation of phosphorylated STAT3 (pSTAT3) levels in *Brca1*-def and *Bard1*-def breast tumor cells and tumor tissue sections.

(A, B) Immunoblot analysis was performed using antibodies against pSTAT3, STAT3 and β -actin (loading control) using lysates from *Flt1i*-expressing (Con) and -deficient (*Flt1i*), talazoparib-resistant ("Res") *Brca1* and *Bard1*-def tumor cells, treated with 50 ng/mL of mouse PGF protein that were used in Fig. 5A, B. (C) Representative images of IHC for pSTAT3 staining in tumor sections from the mice described in Fig. 1 comparing talazoparib-sensitive ("Sen") tumors to talazoparib-resistant ("Res") tumors. Scale bars, 20 μm . (D) Immunostained sections from (C) were quantified using automated QuPath software to identify positively stained cells. For the *Brca1*-def model, $n = 4$ tumors for both Sen and Res. For the *Bard1*-def model, $n = 5$ Sen tumors, and $n = 4$ Res tumors. Data were presented as mean values \pm SEM. P values were determined by a two-tailed, unpaired, Mann-Whitney test. ns; not significant.